

Zero Potential Vorticity Envelopes for the Zonal-Mean Velocity of the Venus/Titan Atmospheres

MICHAEL ALLISON AND ANTHONY D. DEL GENIO

NASA/Goddard Space Flight Center, Institute for Space Studies, New York, New York

WEI ZHOU

Hughes STX Corporation, Institute for Space Studies, New York, New York

(Manuscript received 19 November 1992, in final form 1 July 1993)

ABSTRACT

The diagnostic analysis of numerical simulations of the Venus/Titan wind regime reveals an overlooked constraint upon the latitudinal structure of their zonal-mean angular momentum. The numerical experiments, as well as the limited planetary observations, are approximately consistent with the hypothesis that within the latitudes bounded by the wind maxima the total Ertel potential vorticity associated with the zonal-mean motion is approximately well mixed with respect to the neutral equatorial value for a stable circulation. The implied latitudinal profile of angular momentum is of the form $M \leq M_e(\cos\lambda)^{2/Ri}$, where λ is the latitude and Ri the local Richardson number, generally intermediate between the two extremes of uniform angular momentum ($Ri \rightarrow \infty$) and uniform angular velocity ($Ri = 1$). The full range of angular momentum profile variation appears to be realized within the observed meridional-vertical structure of the Venus atmosphere, at least crudely approaching the implied relationship between stratification and zonal velocity there. While not itself indicative of a particular eddy mechanism or specific to atmospheric superrotation, the zero potential vorticity (ZPV) constraint represents a limiting bound for the eddy-mean flow adjustment of a neutrally stable baroclinic circulation and may be usefully applied to the diagnostic analysis of future remote sounding and in situ measurements from planetary spacecraft.

1. Introduction

The observed circulation of the Venus atmosphere, as revealed by UV cloudtracking, probe Doppler measurements, and spatially resolved thermal wind shears, continues to pose an outstanding problem for the theory of atmospheric dynamics. The various measurements of the zonal-mean flow near the top of the cloud deck, at approximately 65 km altitude, amount to roughly 100 m s⁻¹, over 50 times as fast (but in the same direction) as the rotation of the solid planet below. As first recognized by Leovy (1973), the corresponding thermal wind balance,

$$\frac{\partial}{\partial z} [\tan\lambda U^2 + 2\Omega a \sin\lambda U] = -R \frac{\partial T}{\partial \lambda}, \quad (1)$$

is essentially cyclostrophic, with $U/\cos\lambda \gg \Omega a \approx 1.8$ m s⁻¹. [Here $\hat{z} \equiv \ln(p_0/p)$ is the vertical log-pressure coordinate, λ the latitude, U the zonal velocity, Ω the planetary rotation frequency, a the planetary radius, R the gas constant, and T the temperature.] For illustra-

tion, Leovy presented an exact global solution of the form $U = U_e(\hat{z}) \cos\lambda$, corresponding to uniform angular velocity and a vertically averaged temperature profile $\{\Delta T(\lambda)\} = -[U_e(U_e + 2\Omega a)/2R\hat{z}] \sin^2\lambda$.

Uniform angular velocity has been a featured paradigm of Venus circulation models, corresponding to maximally efficient horizontal eddy diffusion (Gierasch 1975) and the evolved stable state of two-dimensional planetary turbulence (Rossow and Williams 1979). Doppler-tracked probe measurements (Counselman et al. 1980) reveal an atmospheric superrotation at levels below 25 km altitude apparently consistent with the uniform angular velocity profile. The cloud-tracked wind profile (corresponding to altitudes several scale heights higher) more nearly resembles a uniform linear velocity of some 90 m s⁻¹, however, up to about 65° latitude (Rossow et al. 1990), while thermal wind estimates at higher levels near 70 km altitude appear to indicate a state of nearly uniform angular momentum (Newman et al. 1984), with $U \approx 90$ m s⁻¹/cos λ up to about 55°. The tentative inference of global cyclostrophic winds on Titan, based on *Voyager* infrared observations (Flasar et al. 1981) and more recently by the analysis of stellar occultation data (Hubbard et al. 1993), has begun to establish a comparative context for the atmospheric superrotation problem.

Corresponding author address: Dr. Michael Allison, NASA/G155, 2880 Broadway, New York, NY 10025.

The fundamental puzzle presented by these observations is the dynamical maintenance of the implied maximum of *specific angular momentum* $M = a \cos \lambda \times (U + \Omega a \cos \lambda)$ somewhere over the equator, with upper-level winds faster than the planetary rotation. As emphasized by Hide (1969), such a configuration cannot be sustained by downgradient fluxes of angular momentum and is excluded a priori by simple axisymmetric models for the meridional Hadley circulation (e.g., Held and Hou 1980). Gierasch (1975) presented a conceptual solution to the Venus circulation problem with an analytic model in which upward angular momentum transport is accomplished by a meridional circulation cell, with an excess angular momentum at the equator maintained by horizontal eddy transport toward low latitudes. With horizontal eddy fluxes modeled analogously to molecular diffusion, the upgradient transport of angular momentum is consistent with the downgradient transport of the associated angular velocity, as for the Navier–Stokes equations (cf. Read 1986), but the fidelity of this parameterization to the actual behavior of large-scale three-dimensional eddies in the atmosphere is not established. In addition to a strongly anisotropic diffusion of momentum, the Gierasch model also assumes a negligible diffusion of heat, so as not to destroy the horizontal temperature gradient responsible for the meridional overturning and the strong zonal flow. The numerical simulations of Rossow and Williams (1979) demonstrated that barotropic eddies might behave in the prescribed manner, thereby supporting a relaxed state of latitudinally uniform angular velocity. Alternatively, it has been suggested that the Venus atmospheric superrotation could be maintained by the eddy pumping of vertically propagating waves, associated either with the thermal solar tide (e.g., Pechmann and Ingersoll 1984; Leovy 1987; Hou et al. 1990; Newman and Leovy 1992) or topographically forced waves (e.g., Hou and Farrell 1987; Young et al. 1987; Gierasch 1987).

All schemes thus far suggested for either the horizontal or vertical eddy mixing depend upon peculiarly specific prescriptions for the unobserved flux divergences. According to the specific eddy-mixing model adopted by Gierasch, for example, the zonal velocity exhibits an exponential dependence upon an interior vertical eddy viscosity. In the Newman and Leovy model, the acceleration of upper-level motion depends upon the vertically varying competition between the mean flow advection, diurnal and semidiurnal tides, vertical diffusion, and Rayleigh friction. Quite possibly *all* of the variously proposed mechanisms, including surface drag, quasi-barotropic eddy fluxes, thermal tides, and orographically forced gravity waves play a role in the Venus/Titan circulation balance. Available observations, however, do not permit the roles of the various mechanisms to be discriminated. The question thus arises as to whether a general diagnostic constraint on the winds might exist. As originally suggested by

Gierasch (1975), for example, the requisite mixing could represent a downgradient redistribution of potential vorticity. Although the test of this suggestion demands much better data or else its simulation with a three-dimensional nonlinear numerical model, to the extent that it is realized the equilibrated adjustment of angular momentum (and heat) in these atmospheres may be relatively independent of the specific stirring mechanism.

Until recently, numerical general circulation models (GCMs) have not been very successful in the elucidation of this problem. Except by the assumption of somewhat ad hoc momentum sources (e.g., Young and Pollack 1977), these have typically yielded weak or even retrograde (planetary subrotational) winds at the equator (Rossow 1983; Covey et al. 1986; Del Genio and Suozzo 1987). In a new series of numerical experiments with an adapted version of the GISS GCM, however, Del Genio et al. (1993) have shown that an equilibrated atmospheric superrotation is successfully simulated with the incorporation of an optically thick upper cloud layer. The cloud imposes a strong increase of static stability from lower to upper levels in the model, crudely consistent with the in situ Venus observations (Seiff et al. 1980), as well as the vertical stratification assumed by Gierasch (1975). The vertical–meridional structure generated in these experiments suggests an overlooked constraint on the latitudinal distribution of specific angular momentum for equilibrated zonal-mean circulations. The numerical simulations, as well as the limited Venus and Titan observations, are roughly consistent with a latitudinal distribution of Ertel potential vorticity approximately well mixed with respect to the neutral equatorial value for a stable circulation. Although our emphasis in this paper is primarily diagnostic, it is possible that the potential vorticity constraint might eventually serve as a component of a generalized model of quasi-axisymmetric circulation theories (cf. Read 1986) to include the Venus/Titan regime.

2. ZPV envelopes

With the hindsight afforded by the diagnosed structure of GCM simulations of the Venus/Titan regime (cf. Del Genio et al. 1993), as discussed below, we propose that the latitudinal distribution of angular momentum may be usefully constrained in terms of the neutral limiting value of the Ertel (1942) potential vorticity $q \equiv \rho^{-1} \zeta_a \cdot \nabla \Theta$, where ρ is the density, $\zeta_a \equiv \nabla \times (\mathbf{U} + \Omega \times \mathbf{r})$ the vector absolute vorticity, with \mathbf{U} the vector velocity relative to the planetary rotation velocity $\Omega \times \mathbf{r}$, and Θ the potential temperature $\Theta \equiv T(p_0/p)^{R/c_p}$. For zonal-mean motion in a baroclinic atmosphere, also transforming to log-pressure coordinates, q may be represented to the accuracy of the Phillips (1966) approximation as

$$q \approx (g/p) \left[\frac{\partial U}{\partial \hat{z}} \frac{\partial \Theta}{a \partial \lambda} + (\zeta + f) \frac{\partial \Theta}{\partial \hat{z}} \right] \quad (2)$$

(cf. Stevens 1983). Here g is the gravitational acceleration, U the zonal-mean velocity, $\zeta \equiv -(a \cos \lambda)^{-1} \times \partial(U \cos \lambda)/\partial \lambda$ the zonal-mean relative vorticity on the sphere, and $f = 2\Omega \sin \lambda$ the vertical component of planetary vorticity. In terms of the specific angular momentum $M = a \cos \lambda (U + \Omega a \cos \lambda)$,

$$q \approx (g/a^2 p \cos \lambda) \left[\frac{\partial M}{\partial \hat{z}} \frac{\partial \Theta}{\partial \lambda} - \frac{\partial M}{\partial \lambda} \frac{\partial \Theta}{\partial \hat{z}} \right] \\ = (g/a^2 p \cos \lambda) \mathbf{i} \cdot (\nabla \Theta \times \nabla M), \quad (3)$$

where $\nabla \equiv \mathbf{j} \partial/\partial \lambda + \mathbf{k} \partial/\partial \hat{z}$, with \mathbf{i} , \mathbf{j} , and \mathbf{k} denoting unit vectors in the longitudinal, latitudinal, and vertical directions. Then, to the extent that constant M and Θ surfaces are parallel in the meridional-vertical plane, the total Ertel potential vorticity is zero.

According to quasigeostrophic theory, the instability of baroclinic flows is associated with an inflection in the sign of the quasigeostrophic (pseudo) potential vorticity gradient (Charney and Stern 1962). Held (1975) showed that the resulting eddies transport westerly momentum out of the region in which the Charney-Stern criterion is locally satisfied. Hoskins (1974) elucidated the corresponding criterion for nongeostrophic symmetric stability on the “ f plane” (in Cartesian coordinates) appropriate to synoptic-scale motions. More recently, Stevens (1983) has shown that the stability of a negligibly viscous/diabatic prograde planetary circulation (with an equatorial velocity $U_e > -\Omega a$) requires that the Ertel potential vorticity associated with the zonal-mean gradient-balanced flow be positive to the north of the equator and negative to the south. This is a necessary and sufficient criterion. On the equator itself, in the absence of a north-south gradient in the torque or heat source, with q identically zero, stability requires $\partial U/\partial \lambda = 0$. To the extent that baroclinic/barotropic instabilities enforce a nearly vanishing potential vorticity gradient away from the equator, q may be expected to remain small there also. If they do not, stability will ensure that q will at least preserve its sign within each hemisphere. The zero potential vorticity (ZPV) limit implies that

$$\frac{\partial M}{\partial \lambda} \leq \frac{\partial M}{\partial \hat{z}} \frac{\partial \Theta}{\partial \lambda} \left(\frac{\partial \Theta}{\partial \hat{z}} \right)^{-1} \quad (4)$$

(in this form correctly signed for each hemisphere). For gradient-balanced flow, the thermal wind equation (1) implies that

$$\tan \lambda \frac{\partial M^2}{\partial \hat{z}} = -Ra^2 \cos^2 \lambda e^{-R\hat{z}/c_p} \frac{\partial \Theta}{\partial \lambda} \quad (5)$$

so that with (4)

$$\frac{\partial M}{\partial \lambda} \leq -\frac{2M \tan \lambda}{RS} \left(\frac{\partial U}{\partial \hat{z}} \right)^2 = -\frac{2M \tan \lambda}{\text{Ri}}, \quad (6)$$

where $S \equiv e^{-R\hat{z}/c_p} \partial \Theta/\partial \hat{z} = \partial T/\partial \hat{z} + RT/c_p$ is the static stability parameter and $\text{Ri} \equiv RS/(\partial U/\partial \hat{z})^2$ the Richardson number. The stability constraint (6) implies a maximum latitudinal shear for the zonal velocity given as

$$\partial U/\partial \lambda \leq U(1 - 2/\text{Ri}) \tan \lambda + 2\Omega a(1 - 1/\text{Ri}) \sin \lambda. \quad (7)$$

To the extent that the latitudinal variation of the Richardson number can be neglected, (6) immediately integrates to

$$M \leq M_e (\cos \lambda)^{2/\text{Ri}} \equiv M_{\max}, \quad (8)$$

where $M_e \equiv a(U_e + \Omega a)$ is the equatorial value for the specific angular momentum. The corresponding envelope for the zonal-mean velocity is

$$U_{\max} = (U_e + \Omega a)(\cos \lambda)^{2/\text{Ri} - 1} - \Omega a \cos \lambda, \quad (9)$$

where in general both U_e and Ri vary with altitude. (While strictly artificial, the assumption of a uniform Richardson number at each level is adopted for convenience and the purpose of illustration.) Three special cases are of particular interest.

For $\text{Ri} = 1$, $M_{\max} = M_e \cos^2 \lambda$ and

$$U_{\max} = U_e \cos \lambda, \quad (10)$$

as for uniform angular velocity, with an associated latitudinal temperature contrast with respect to the equator, vertically averaged up to a height \hat{z} , given as

$$\{\Delta T(\lambda)\}_{\max} = -[U_e(U_e + 2\Omega a)/2R\hat{z}] \sin^2 \lambda, \quad (11)$$

assuming a surface velocity negligible compared to U_e .

For $\text{Ri} = 2$, $M_{\max} = M_e \cos \lambda$ and

$$U_{\max} = U_e + \Omega a(1 - \cos \lambda), \quad (12)$$

corresponding to uniform absolute velocity, with

$$\{\Delta T(\lambda)\}_{\max} = [(U_e + \Omega a)^2/R\hat{z}] \ln(\cos \lambda) \\ + [(\Omega a)^2/2R\hat{z}] \sin^2 \lambda. \quad (13)$$

For $\text{Ri} \rightarrow \infty$, $M_{\max} = M_e$, corresponding to uniform angular momentum and zero absolute vorticity, with

$$U_{\max} = (U_e + \Omega a \sin^2 \lambda)/\cos \lambda \quad (14)$$

and

$$\{\Delta T(\lambda)\}_{\max} = -[(U_e + \Omega a)^2 - (\Omega a)^2 \cos^2 \lambda] \\ \times \tan^2 \lambda / 2R\hat{z}. \quad (15)$$

Of the three special cases, only the $\text{Ri} = 1$ case is “equivalent barotropic” in the sense that the zonal-mean flow is of the separable form $U(\lambda, \hat{z}) = U_e(\hat{z}) \cdot F(\lambda)$, that is, with a horizontal motion field entirely self-similar with altitude. This is consistent with the similarity of the corresponding uniform angular velocity profile with the Rossow and Williams (1979) experiments demonstrating its development as

the relaxed state of barotropic planetary turbulence. Only the (fixed) $Ri = 2$ case has a vertical wind shear and static stability uniform with latitude. Wherever the Richardson number is large, the limiting profiles of velocity and temperature are relatively insensitive to the artificial assumption of its uniformity with latitude, owing to its reciprocal dependence in the ZPV relations. These represent a generalization of the corresponding expressions for velocity and temperature in the axisymmetric model of Held and Hou (1980), for which the purely advective redistribution of angular momentum by the mean meridional flow demands that $U_e = 0$ (in order for M to adhere to the value imposed at the equatorial surface). According to the zero potential vorticity constraint, however, $\partial M / \partial |\lambda| < 0$ at all levels for which $|\partial U / \partial z| \neq 0$ (and $1 \leq Ri < \infty$).

3. Comparison with GCM experiments

Figure 1 displays constant angular momentum and potential temperature contours in the meridional-vertical plane for the GCM simulations of a dry terrestrial atmosphere with a 16-day planetary rotation period and an imposed statically stable upper cloud deck, with and without the inclusion of parameterized stratospheric wave drag (Del Genio et al. 1993). While not precisely parallel, the similarity in the shape of the M and Θ surfaces is evident at latitudes below the corresponding angular velocity maxima, at about 60° , implying a relatively well mixed region of potential vorticity. The stippled areas in these figures indicate regions where the potential vorticity gradient is slightly negative, corresponding to intervals where the M and Θ contours are increasingly parallel with latitude, thereby satisfying the necessary condition for barotropic/baroclinic instability. As diagnosed by Del Genio et al., the dynamical structure of these simulations is maintained by an equatorward transport of angular momentum within the same regions by quasi-barotropic eddies (cf. their Fig. 8b). The identification of barotropic instability is based on the existence of equatorward eddy momentum fluxes on the equatorial side of the midlatitude jets, well-mixed absolute vorticity at these locations, large barotropic conversion and negative baroclinic conversion, and negligible eddy heat transports. Equatorial flux divergence maxima and small-scale meridional cells characteristic of inertial instability are not evident in the GCM, while other proposed superrotation mechanisms such as thermal tides and small-scale orographic gravity waves are excluded by the absence of a diurnal cycle and topography in the GCM. The quasi-barotropic eddy processes evidently work toward the effacement of strong gradients in the zonal-mean Ertel potential vorticity, as anticipated by Gierasch (1975), especially within and just below the cloud deck, where the eddies are most active.

ZPV cannot be expected to exist at all levels, particularly in the vicinity of top and bottom boundaries,

where dissipative processes and special matching conditions may prevail instead. At lower levels in the model simulation, where the stippled areas overlap the equator and the M surfaces cut under rather than over the intersected Θ surfaces toward higher latitudes, the potential vorticity is actually negative in the northern hemisphere (positive in the southern hemisphere). Although these regions satisfy the inertial instability criterion for an inviscid adiabatic circulation, their confinement to levels roughly coincident with the convective and dissipative boundary layer precludes their diagnosis as the site of purely inertial eddies and at any rate are well below the atmospheric superrotation aloft. The parallelism of M and Θ surfaces in these experiments also breaks down above the 200-mb level increasingly with latitude, with and without the inclusion of stratospheric wave drag, corresponding to large values of q (positive to the north, negative to the south of the equator) and q_y , uniformly large, consistent with the absence of strong eddy transports in these regions.

As noted by Del Genio et al. (1993), the velocity profiles for the cloud-level flow in their experiments T1 and T3 (with and without upper-level wave drag) closely match the limiting ZPV profile for $Ri \approx 2$, specified by Eq. (12). The approximate $\cos \lambda$ variation of the specific angular momentum implied by Eq. (8) for $Ri \approx 2$ is clearly evident in Fig. 1 (showing roughly a factor of 2 reduction between the equator and 60° latitude, for example). The $\ln(\cos \lambda)$ dependence of the temperature contrast specified by (13) for the cyclostrophic regime ($U_e > \Omega a$), increasing in magnitude by a factor of approximately 5 between 30° and 60° latitude, is in good agreement with the potential temperature contrast displayed in Fig. 1 at the 600-mb ($z \approx 0.5$) level, for example. The uniform static stability feature of the $Ri = 2$ regime may account for its approximate realization in the GCM experiments of Del Genio et al. (1993), again clearly evident in Fig. 1, where the stratification is essentially imposed by a uniform solar-absorbing cloud deck.

Figure 2 displays contoured fields of the local Richardson number computed by finite differences of the GCM output. Although T1 shows regions of relatively large Richardson number between the 700- and 900-mb levels as well as above 300–400 mb, it is elsewhere smaller than 10 within the latitudes bounded by the jets near 70° . Near the peak level for the equatorward transport of angular momentum by eddies, $Ri \approx 2$ –5 within 60° latitude. For the more strongly superrotating experiment T3, absent stratospheric drag, the Richardson number is less than 5 throughout the region within the jet latitudes and below 425 mb and less than 3 over much of this region.

Numerical estimates of the GCM potential vorticity indicate that between 300 and 900 mb and within 60° latitude, q at a given level is everywhere less than about 20% of its value near the pole, and in this sense actually approximates the “zero” potential vorticity limit. This

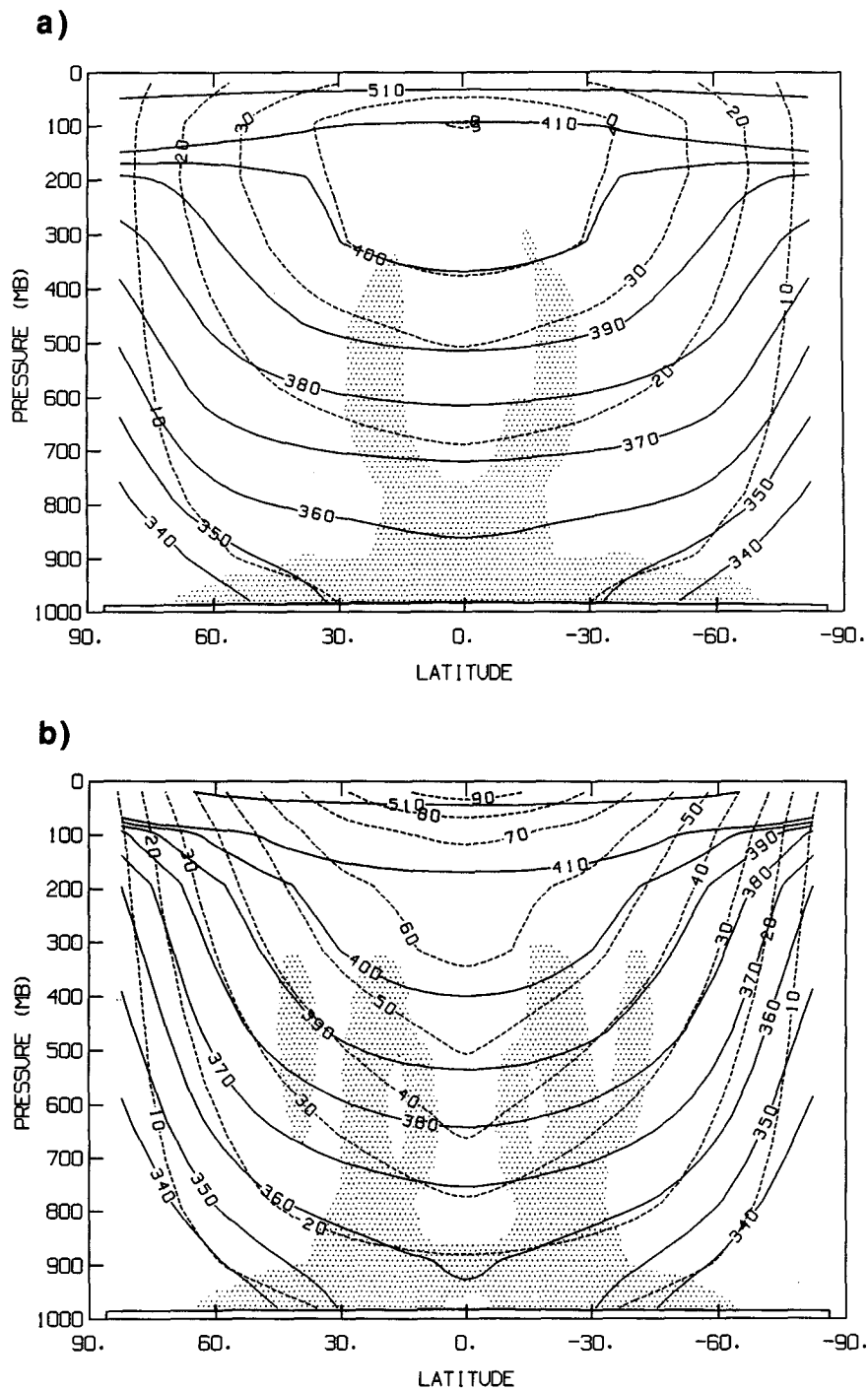


FIG. 1. Contours of constant specific angular momentum ($10^7 \text{ m}^2 \text{ s}^{-1}$), shown as dashed curves, and constant potential temperature (K), shown as solid curves, in the meridional-vertical plane for the equilibrated zonal-mean circulation generated in the terrestrial GCM experiments by Del Genio et al. (1993) with a planetary rotation period of 16 days and an imposed statically stable upper-level cloud deck. Panel (a) displays the results of experiment T1, including stratospheric wave drag and a closed upper-level jet. Panel (b) displays the results of experiment T3, without stratospheric wave drag, for which the specific angular momentum increases monotonically with altitude. Stippled areas correspond to regions with a negative latitudinal PV gradient.

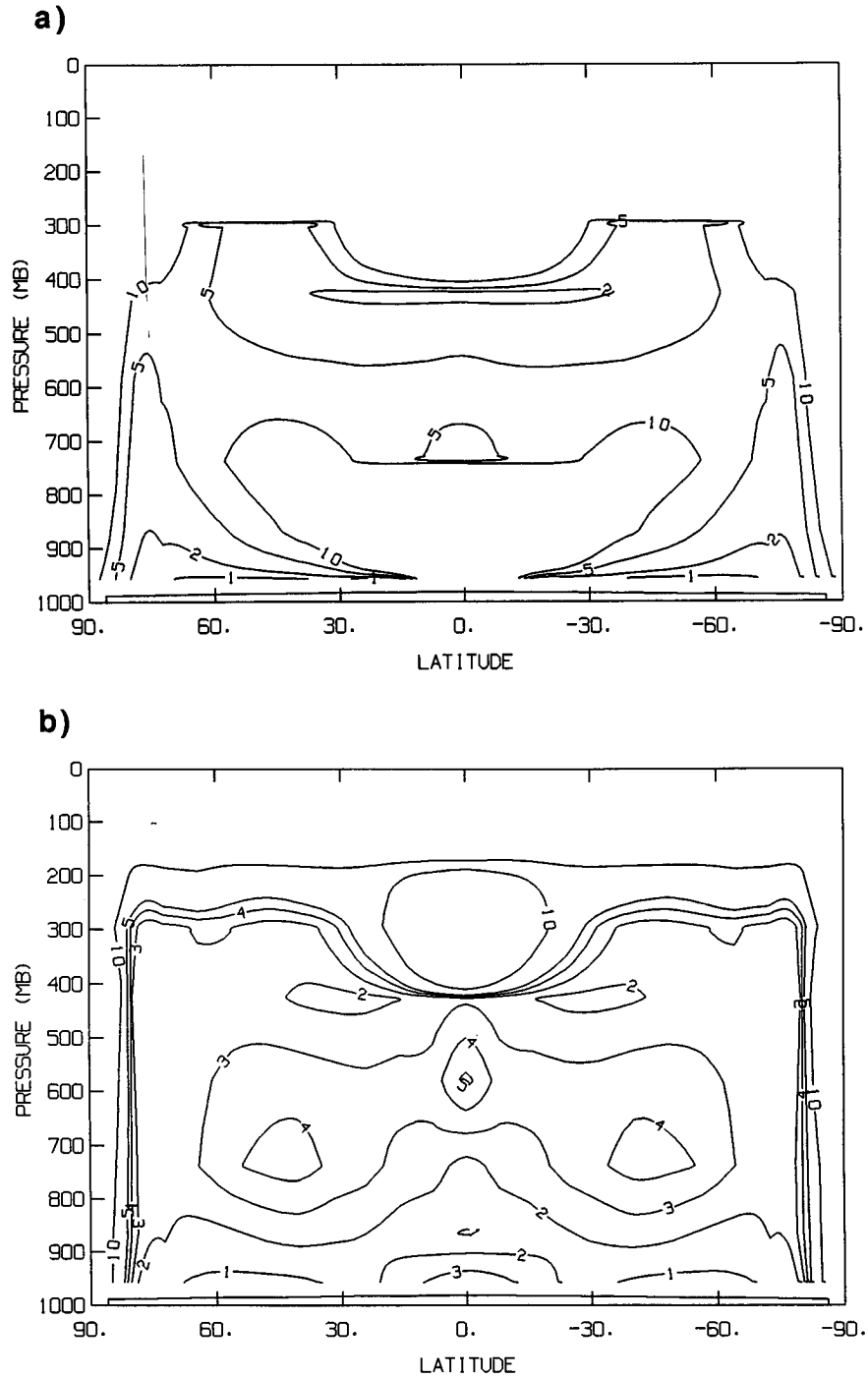


FIG. 2. Contours of constant Richardson number for the equilibrated zonal-mean circulation of the GCM experiments by Del Genio et al. (1993), with a planetary rotation period of 16 days and an imposed statically stable upper-level cloud deck. Panel (a) corresponds to experiment T1 (with stratospheric wave drag), contoured at $Ri = 1, 2, 5,$ and 10 . Panel (b) corresponds to T3 (without stratospheric wave drag) contoured at $Ri = 1, 2, 3, 4, 5,$ and 10 .

configuration of steep PV gradients near the pole, surrounded by relatively homogeneous potential vorticity at lower latitudes, may be analogous to the polar vortex region in the earth's winter stratosphere, bounding the so-called surf zone of planetary wave breaking (cf. Butchart and Remsberg 1986). Laboratory simulations of prograde planetary jets (cf. Sommeria et al. 1989) reveal a similar isolation of steep PV gradients within an annular region close to the rotation axis, surrounded by nearly homogeneous potential vorticity. Except where $Ri < 2$, the ZPV profiles obviously cannot extend all the way to the pole, where the implied expressions for velocity and temperature would diverge. Again, the ZPV profiles are best regarded as limiting envelopes, likely to approximate the actual velocity and temperature structure only within the latitudes and altitudes bounded by the jet maxima, as yet only crudely defined for Venus, where they may also vary diurnally, and as yet only tentatively inferred on Titan, where they likely vary with the seasons.

Experiments with another Titan GCM currently under development by Hourdin et al. (1992) also show superrotational zonal mean winds apparently constrained by the uniform angular momentum profile at upper simulation levels where the Richardson number is presumably large. Although their preliminary report does not include a quantitative analysis of the responsible flux transports, their diagnosis of the zonally averaged absolute vorticity field also includes regions satisfying the necessary condition for barotropic instability.

4. Comparison with the Venus/Titan observations

The assembled vertical–meridional structure measurements for Venus from several spacecraft at selected levels may offer an example of each of the three special ZPV envelopes outlined above. Figure 3 displays velocities at three different altitudes as inferred from *Pioneer Venus* measurements along with the special ZPV profile that best matches the observations. Accuracy and sampling limitations preclude sufficiently precise estimates of Ri to validate the ZPV diagnosis, but the gross features of the observed variations of $\partial U/\partial \lambda$ and Ri between the lower and upper Venus atmosphere are at least suggestive of control by PV mixing. At 25 km altitude, in situ probe Doppler-tracking measurements (Counselman et al. 1980) at three locations appear to match a uniform angular velocity profile (10), as indicated by the dashed curve. Probe atmospheric structure measurements at these levels show a nearly adiabatic lapse rate (Seiff et al. 1980) consistent with a roughly unitary Richardson number. (Precise verification is difficult, involving the estimation of temperature and velocity derivatives near the limit of the local deviations in the data.)

At the UV cloud level, temporally averaged feature tracking measurements reveal a roughly uniform ve-

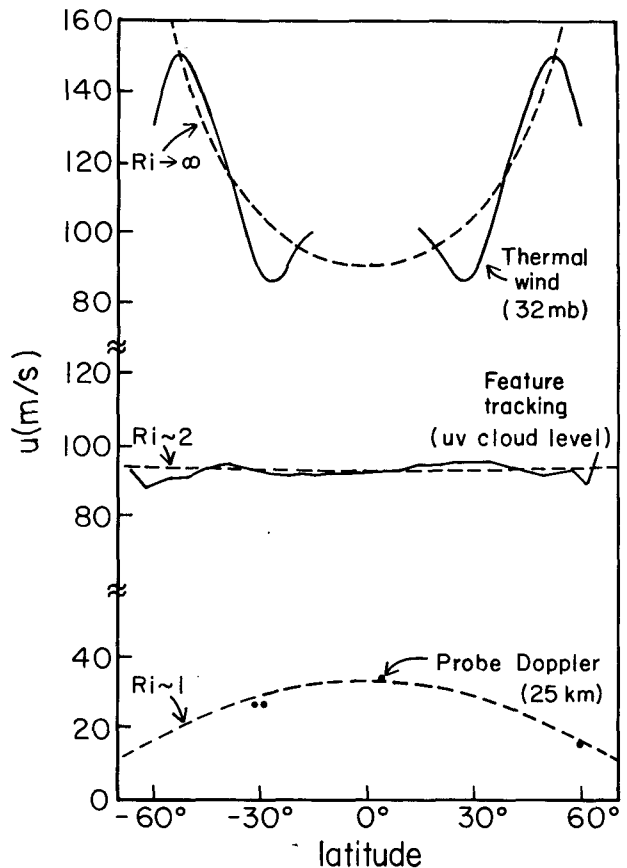


FIG. 3. Latitudinal profiles of zonal mean velocity at three different levels in the Venus atmosphere. The four dots at the 25-km level correspond to probe Doppler wind measurements (Counselman et al. 1980). The solid curve at the UV cloud level is based on feature tracking measurements (Rossow et al. 1990), while that at the 32-mb level is inferred from the thermal wind shear analysis of radio occultation soundings, with data from North and South hemispheres folded together (Newman et al. 1984). The dashed curves correspond to the ZPV envelopes for $Ri = 1, 2, \text{ and } \infty$ as indicated.

locity within 60° latitude nearly indistinguishable from the ZPV profile (12) for $Ri = 2$. These observations pertain to an altitude just above the highest probe Doppler-tracking levels, but for very different local solar times. The cloud-tracked winds are located primarily within a few hours of local noon, while the probes sampled the morning terminator and night side of Venus. At the probe longitudes, the nearly adiabatic (and presumably small Ri) middle cloud layer terminates near 60 km, with rapidly increasing Ri above, while on the day side the static stability is poorly constrained. The meridional shear in the cloud-tracked winds varies with local solar time, maximized in the morning hemisphere at a value consistent with the ZPV limit for $Ri \sim 4\text{--}5$ [cf. Fig. 12 of Del Genio and Rossow (1990)], in somewhat better agreement with the probe inferences. Interannual variations also result in more pronounced jets (consistent with larger Ri) in certain ep-

ochs than for the accumulated mean displayed in Fig. 3. Although a moderate value for the Richardson number cannot be confirmed with the available data at these levels, it should be remembered that the ZPV profile for a fixed (but possibly large) Ri strictly corresponds only to an upper limit for the zonal velocity profile. It is also of interest to note that the dominant planetary-scale “Y” feature at the UV cloud level, identified by Del Genio and Rossow (1990) as a 4-day Kelvin wave, is itself a nonaxisymmetric mode of zero potential vorticity (cf. Stevens et al. 1990).

At the 32-mb (~ 70 km) level, integrated thermal winds derived from *Pioneer Venus* radio occultation data by Newman et al. (1984), based on the combined data for both hemispheres, imply the indicated latitudinal zonal wind profile in Fig. 3 (solid curve), plotted in comparison with the uniform angular momentum profile (dashed curve) corresponding to $Ri \rightarrow \infty$. This level closely corresponds to the jet core in the vertical profile of the derived thermal wind, where $\partial U/\partial z \rightarrow 0$, and the Richardson number may be accurately regarded as large there. Although Newman et al. emphasize their uncertainty regarding the displayed “sag” in the latitudinal wind profile near 30° latitude (and indeed such a profile is inertially unstable), its overall variation is at least crudely consistent with uniform angular momentum. Qualitatively similar results for the zonal thermal wind field at these levels are presented by Taylor et al. (1988), based on two months of independent global measurements from an infrared sounder on the *Pioneer Venus Orbiter*.

The tentative diagnosis of global cyclostrophic winds on Titan associated with the ~ 20 -K equator-to-pole contrast in stratospheric brightness temperatures inferred by the *Voyager* infrared experiment (Flasar et al. 1981; Flasar and Conrath 1990) presents an important target for further observational and model analysis. The recent analysis of an earth-based stellar occultation by Titan, presented by Hubbard et al. (1993), provides an independent inference of the upper atmospheric velocity as a function of latitude. Their results imply a zonal wind at the 0.25-mb level (where the Richardson number is almost certainly large, owing to the strongly stable stratification there) varying from some 80 m s^{-1} near the equator to more than 170 m s^{-1} at 60° latitude, in good agreement with uniform angular momentum.

The upcoming *Cassini/Huygens* mission to Titan will combine further global orbiter remote sensing observations with direct probe Doppler tracking and in situ pressure-temperature measurements. The measured vertical profile of temperature by the Huygens Atmospheric Structure Instrument will define the static stability structure that, together with the measured vertical shear afforded by the Doppler Wind Experiment (Atkinson et al. 1990), will provide a determination of the Richardson number. Measured winds and temperatures at each probe descent level could then be interpreted as ZPV envelopes to be checked against inde-

pendent remote sensing measurements from the *Cassini Orbiter*.

5. Discussion

Lindzen (1990) has suggested that “. . . the climate is largely determined by processes which mix potential vorticity—among which processes baroclinic instability is a major contributor.” Lindzen and Farrell (1980) established the plausibility of this hypothesis with a parameterization of the global heat transport in the earth’s atmosphere, based on the assumption that the eddy fluxes be only just sufficient to neutralize the flow, as prescribed by the requirement that the meridional gradient of potential vorticity not change its sign. Their results produced a remarkable agreement between predicted temperatures and observations, fairly independent of the specific choice of radiative forcing parameters, despite their neglect of fluxes by oceanic transports and stationary waves. Lindzen and Farrell conjectured that the baroclinic eddies in the earth’s atmosphere may therefore be regarded as a climatic regulator of the (thermal) “voltage” between equator and pole, with the competing processes simply taking up the role otherwise played by baroclinic fluxes in their absence.

A similar principle of potential vorticity homogenization may be of controlling importance for the cyclostrophic circulations of Venus and Titan involving latitudinal and/or vertical transports of angular momentum. This approach to the analysis of these atmospheres has so far received little attention, however, possibly owing to a lack of sufficiently detailed observations and model simulations. In the GCM experiments reported by Del Genio et al. (1993), potential vorticity is smoothed toward its neutral equatorial value by the unstable adjustment of quasi-barotropic eddies. The self-consistent confirmation of the ZPV diagnostics with the latitudinal and vertical structure of the equilibrated GCM fields demonstrates the plausible relevance of this principle to a three-dimensional cyclostrophic circulation. While the ZPV limit corresponds to the threshold of inertial instability, we emphasize that this need not be (and in the case of the GCM evidently is not) the responsible homogenization process. ZPV does not by itself provide a complete account of the circulation or even enforce an equatorial superrotation. The real Venus/Titan circulation may also include transports by thermotidal and inertia-gravity waves, which in principle might also act to homogenize the potential vorticity, thereby yielding zonal wind profiles approaching the ZPV limit. Although our understanding of these circulation systems will not be complete until we have identified the specific eddy processes responsible for their maintenance, the ZPV limit nevertheless represents a useful bounding template for the analysis of planetary structure data as well as the diagnosis of model simulations.

Acknowledgments. We thank Peter Gierasch and an anonymous referee for several thoughtful and helpful comments and William Rossow and Larry Travis for stimulating discussions. Figure 3 was drafted by Jose Mendoza. This research was supported by the NASA Planetary Atmospheres Program managed by Jay Bergstralh.

REFERENCES

- Atkinson, D. H., J. B. Pollack, and A. Seiff, 1990: Measurement of a zonal wind profile on Titan by Doppler tracking of the Cassini entry probe. *Radio Sci.*, **25**, 865–881.
- Butchart, N., and E. E. Remsburg, 1986: The area of the stratospheric polar vortex as a diagnostic for tracer transport on an isentropic surface. *J. Atmos. Sci.*, **43**, 1319–1339.
- Charney, J. G., and M. E. Stern, 1962: On the instability of internal baroclinic jets in a rotating atmosphere. *J. Atmos. Sci.*, **19**, 169–82.
- Counselman, C. C., S. A. Gourevitch, R. W. King, and G. B. Lioriot, 1980: Zonal and meridional circulation of the lower atmosphere of Venus determined by radio interferometry. *J. Geophys. Res.*, **85**, 8026–8030.
- Covey, C., E. J. Pitcher, and J. P. Brown, 1986: General circulation model simulations of superrotation in slowly rotating atmospheres: Implications for Venus. *Icarus*, **66**, 380–396.
- Del Genio, A. D., and W. B. Rossow, 1990: Planetary-scale waves and the cyclic nature of cloud top dynamics on Venus. *J. Atmos. Sci.*, **47**, 293–318.
- , W. Zhou, and T. P. Eichler, 1993: Equatorial superrotation in a slowly rotating GCM: Implications for Titan and Venus. *Icarus*, **101**, 1–17.
- Ertel, H., 1942: Ein Neuer hydrodynamischer Wirbelsatz. *Meteor. Z.*, **59**, 271–281.
- Flasar, F. M., and B. J. Conrath, 1990: Titan's stratospheric temperatures: A case for dynamical inertia? *Icarus*, **85**, 346–354.
- , R. E. Samuelson, and B. J. Conrath, 1981: Titan's atmosphere: Temperature and dynamics. *Nature*, **292**, 693–698.
- Gierasch, P. J., 1975: Meridional circulation and the maintenance of the Venus atmospheric rotation. *J. Atmos. Sci.*, **32**, 1038–1044.
- , 1987: Waves in the atmosphere of Venus. *Nature*, **328**, 510–512.
- Held, I. M., 1975: Momentum transport by quasi-geostrophic eddies. *J. Atmos. Sci.*, **32**, 1494–1497.
- , and A. Y. Hou, 1980: Nonlinear axially symmetric circulations in a nearly inviscid atmosphere. *J. Atmos. Sci.*, **37**, 515–533.
- Hide, R., 1969: Dynamics of the atmospheres of the major planets with an appendix on the viscous boundary layer at the rigid bounding surface of an electrically-conducting rotating fluid in the presence of a magnetic field. *J. Atmos. Sci.*, **26**, 841–853.
- Hoskins, B. J., 1974: The role of potential vorticity in symmetric stability and instability. *Quart. J. Roy. Meteor. Soc.*, **100**, 480–482.
- Hou, A. Y., and B. F. Farrell, 1987: Superrotation induced by critical-level absorption of gravity waves on Venus: An assessment. *J. Atmos. Sci.*, **44**, 1049–1061.
- , S. B. Fels, and R. M. Goody, 1990: Zonal superrotation above Venus's cloud base induced by the semidiurnal tide and the mean meridional circulation. *J. Atmos. Sci.*, **47**, 1894–1901.
- Hourdin, F., P. Le Van, O. Talagrand, R. Courtin, D. Gautier, and C. P. McKay, 1992: Numerical simulation of the circulation of the atmosphere of Titan. *Symposium on Titan*, ESA SP-338, 101–106. [Copies available from ESA Publications Division, ESTEC, Noordwijk, The Netherlands.]
- Hubbard, W. B., and 45 co-authors, 1993: The occultation of 28 Sgr by Titan. *Astron. Astrophys.*, **269**, 541–563.
- Leovy, C. B., 1973: Rotation of the upper atmosphere of Venus. *J. Atmos. Sci.*, **30**, 1218–1220.
- , 1987: Zonal winds near Venus' cloud top level: An analytic model of the equatorial wind. *Icarus*, **69**, 193–201.
- Lindzen, R. S., 1990: *Dynamics in Atmospheric Physics*. Cambridge University Press, 310 pp.
- , and B. Farrell, 1980: The role of polar regions in global climate and a new parameterization of global heat transport. *Mon. Wea. Rev.*, **108**, 2064–2079.
- Newman, M., and C. Leovy, 1992: Maintenance of strong rotational winds in Venus' middle atmosphere by thermal tides. *Science*, **257**, 647–650.
- , G. Schubert, A. J. Kliore, and I. R. Patel, 1984: Zonal winds in the middle atmosphere of Venus from Pioneer Venus radio occultation data. *J. Atmos. Sci.*, **41**, 1901–1913.
- Pechmann, J. B., and A. P. Ingersoll, 1984: Thermal tides in the atmosphere of Venus: Comparison of model results with observations. *J. Atmos. Sci.*, **41**, 3290–3313.
- Phillips, N. A., 1966: The equations of motion for a shallow rotation atmosphere and the "traditional approximation." *J. Atmos. Sci.*, **23**, 626–628.
- Read, P. L., 1986: Super-rotation and diffusion of axial angular momentum. II. A review of quasi-axisymmetric models of planetary atmospheres. *Quart. J. Roy. Meteor. Soc.*, **112**, 253–272.
- Rossow, W. B., and G. P. Williams, 1979: Large-scale motion in the Venus stratosphere. *J. Atmos. Sci.*, **36**, 377–389.
- , A. D. Del Genio, and T. Eichler, 1990: Cloud-tracked winds from Pioneer Venus OCPP images. *J. Atmos. Sci.*, **47**, 2053–2084.
- Schubert, G., C. Covey, A. Del Genio, L. S. Elson, G. Keating, A. Seiff, R. E. Young, J. Apt, C. C. Counselman III, A. J. Kliore, S. S. Limaye, H. E. Revercomb, L. A. Sromovsky, V. E. Suomi, F. Taylor, R. Woo, and U. von Zahn, 1980: *J. Geophys. Res.*, **85**, 8007–8025.
- Seiff, A., D. B. Kirk, R. E. Young, R. C. Blanchard, J. T. Findlay, G. M. Kelly, and S. C. Sommer, 1980: Measurements of thermal structure and thermal contrasts in the atmosphere of Venus and related dynamical observations: Results from the four Pioneer Venus probes. *J. Geophys. Res.*, **85**, 7903–7933.
- Sommeria, J., S. D. Meyers, and H. L. Swinney, 1989: Laboratory model of a planetary eastward jet. *Nature*, **337**, 58–61.
- Stevens, D. E., 1983: On symmetric stability and instability of zonal mean flows near the equator. *J. Atmos. Sci.*, **40**, 882–893.
- , H.-C. Kuo, W. H. Schubert, and P. E. Ciesielski, 1990: Quasi-balanced dynamics in the tropics. *J. Atmos. Sci.*, **47**, 2262–2273.
- Taylor, F. W., P. J. Gierasch, P. L. Read, and R. Hide, 1988: The dynamics of planetary atmospheres. *Sci. Prog. Oxf.*, **72**, 421–450.
- Young, R. E., and J. B. Pollack, 1977: A three-dimensional model of dynamical processes in the Venus atmosphere. *J. Atmos. Sci.*, **34**, 1315–1351.
- , R. L. Walterscheid, G. Schubert, A. Seiff, V. M. Linkin, and A. N. Lipatov, 1987: Characteristics of gravity waves generated by surface topography on Venus: Comparison with the VEGA balloon results. *J. Atmos. Sci.*, **44**, 2628–2639.